Weakly Self-Assembled [6]helicenes: Circularly Polarized Light and Spin Filtering Properties

Rafael Rodríguez, Cristina Naranjo, Anil Kumar, Kais Dhbaibi, Paola Matozzo, Franck Camerel, Nicolas Vanthuyne, Rafael Gomez-Ramirez, Ron Naaman, Luis Sanchez, et al.

Weakly Self-Assembled [6]Helicenes: Circularly Polarized Light and Spin Filtering Properties

Rafael Rodríguez,[⊥a] Cristina Naranjo,[⊥b] Anil Kumar,[c] Kais Dhbaibi,[a] Paola Matozzo,[a] Franck Camerel,[a] Nicolas Vanthuyne,[d] Rafael Gómez,[a] Ron Naaman,*[c] Luis Sánchez,*[b] and Jeanne Crassous,*[a]

[a] Dr. R. Rodríguez, Dr. K. Dhbaibi, P. Matozzo, Dr. F. Camerel, Dr. J. Crassous
Institut des Sciences Chimiques de Rennes
University of Rennes, CNRS, ISCR
UMR 6226, F-35000 Rennes, France
E-mail: Jeanne.crassous@univ-rennes1.fr

[b] C. Naranjo, Prof. Dr. R. Gómez, Prof. Dr. L. Sánchez
Departamento de Química Orgánica, Facultad de Ciencias Químicas
Universidad Complutense de Madrid
Ciudad Universitaria s/n; 28040, Madrid, Spain
E-mail: lusamar@ucm.es

[c] A. Kumar, Prof. Dr. R. Naaman
Department of Chemical and Biological Physics
Weizmann Institute of Science
Rehovot 76100, Israel
E-mail: ron.naaman@weizmann.ac.il

[d] N. Vanthuyne
Aix Marseille Université
Centrale Marseille, CNRS, iSm2
UMR 7313, Marseille 13397, France

Supporting information for this article is given via a link at the end of the document.

Abstract: We report herein on the self-assembling features, chiroptical activity, and spin filtering properties of 2,15- and 4,13-disubstituted [6]helicenes decorated in their periphery with 3,4,5-tris(dodecyloxy)-*N*-(4-ethynylphenyl)benzamide moieties. The weak non-covalent interaction between these units conditions the corresponding circularly polarized luminescence and spin polarization. The self-assembly is overall weak for these [6]helicene derivatives that, despite the formation of H-bonding interactions between the amide groups present in the peripheral moieties, shows very similar chiroptical properties both in the monomeric or aggregated states. This effect could be explained by considering the steric effect that these groups could generate in the growing of the corresponding aggregate formed. Importantly, the self-assembling features also condition chiral induced spin selectivity (CISS effect), with experimental spin polarization (SP) values found between 35-40% for both systems, as measured by magnetic-conducting atomic force microscopy (AFM) technique.

Introduction

Helicenes, ortho-fused aromatic compounds adopting helical chirality,[1] have been reported as useful building blocks with efficient circularly polarized luminescence (CPL) activity[2] and spin filtering capabilities[3] that make them complementary candidates to some other systems like metal complexes,[4] small organic luminescent molecules[5] or nanographenes,[6] for the development of new technological applications like data storage, biological sensing or spintronic devices.[7] Importantly, the formation of organized active layers, in which the self-assembly of the above-mentioned molecular systems by non-covalent interactions is crucial, plays a pivotal role in the achievement of these technological applications. Taking into account that both CPL and spin-filtering effect require the participation of chiral species, chiral supramolecular polymers can emerge as an interesting benchmark to build up highly organized, functional chiral assemblies.[8] A large number of chiral supramolecular polymers are formed by the self-assembly of planar aromatic moieties like BTAs,[9] PBIs,[10] π-conjugated oligomers,[11] or porphyrins[12] that would yield a racemic mixture of helical structures. Therefore, enantioenriched helical supramolecular polymers can be achieved by: i) an efficient transfer of asymmetry from the point chirality embedded in the peripheral side chains,[9-12] ii) the co-assembly of two enantiomers in different ratio (majority rules) or a chiral/achiral mixture of referable moieties (Sergeants and Soldiers),[11,13] iii) using chiral additives,[14] or iv) irradiating with CPL.[15] Much less investigated are those chiral supramolecular polymers in which the self-assembling units are 3D moieties displaying axial or inherent chirality. These distorted and rigid geometries prevent a straightforward self-assembly.[16-18] Atropoisomers[16] and helicenes[17] are paradigmatic chiral, non-planar moieties that upon self-assembly generate chiral supramolecular polymers. Very recently, we have reported on the outstanding CPL activity and spin filtering effect of supramolecular polymers formed by the self-assembly of 2,15- and 4,13-disubstituted [6]helicenes endowed with four amide functional groups that favors the supramolecular interaction by the formation of a fourfold array of H-bonding interactions. Either the final properties (luminescence dissymmetry factors, g_{lum}, and spin filtering effect) and the supramolecular polymerization mechanism strongly depends on the substitution pattern of the [6]helicene backbone. Thus, the 2,15-disubstituted [6]helicene forms chiral supramolecular polymers by following an isodesmic mechanism, presents CPL activity of the same sign as the monomeric species and a remarkable spin polarization

percentage (SP%) of 80 %. On the contrary, the 4,13-disubstituted [6]helicene forms chiral supramolecular polymers by following a cooperative mechanism, the CPL activity of these supramolecular polymers exhibits an opposite sign than that of the monomeric species and a SP% of 60 %.[18]

Here we expand our studies on the formation of self-assembled, functional species from 2,15- and 4,13-disubstituted [6]helicenes by decorating their periphery with two 3,4,5-tris(dodecyloxy)-*N*-(4-ethynylphenyl)benzamide moieties (compounds **1** and **2** in Figure 1). These peripheral fragments strongly condition the self-assembly of these distorted systems and, consequently, the corresponding CPL activity and spin filtering. Thus, both [6]helicenes **1** and **2** present a weak tendency to form aggregated species that is especially weak in compound **2**. In good agreement with our previous studies,[18] the [6]helicenes **1** self-assemble in a head-to-tail manner but the [6]helicenes **2** do it in a head-to-head fashion (Figure 1b and 1c). These weak self-assembly ability results in a very similar emissive and dichroic response for both the monomeric and aggregated species. Importantly, both [6]helicenes **1** and **2** present a noticeable spin filtering effect (Figure 1b and 1c). The results presented herein corroborate the influence of the 3,4,5-tris(dodecyloxy)-*N*-(4-ethynylphenyl)benzamide moiety, which has been demonstrated to induce anticooperative supramolecular polymerization attenuated by the chain growth[19] and contribute to shed light on the structural elements participating in the achievement of functional, supramolecular polymers.

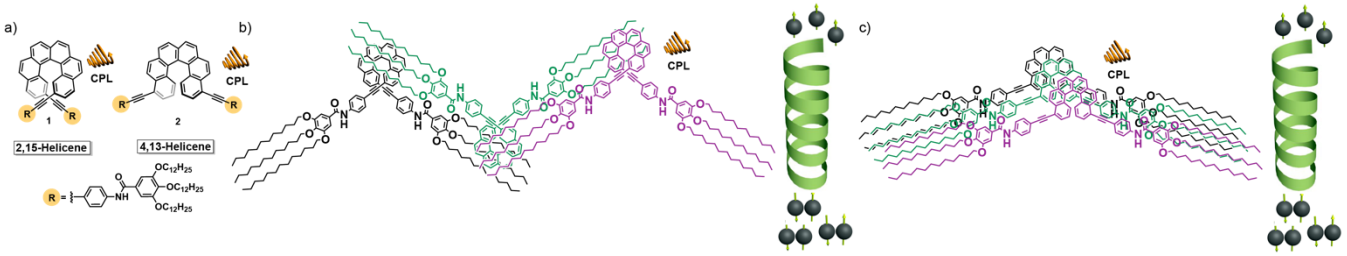

Figure 1. (a) Chemical structures of [6]helicenes **1** and **2**. Schematic illustration of the (b) head-to-tail self-assembly of **1** and the (c) head-to-head self-assembly of **2**. All the enantioenriched species, both in their monomeric or aggregated states, act as CPL emitters with no changes in the CPL sign. The aggregated species of **1** and **2** present spin filtering effects.

Results and Discussion

Synthesis and self-assembling features. In good agreement with our previous study,[18] the [6]helicenes **1** and **2** in their racemic form were prepared by carrying out a twofold C-C cross-coupling Sonogashira reaction between the racemic 2,15- and 4,13-bis-ethynyl-carbo[6]helicene building blocks[20] and 3,4,5-tris(dodecyloxy)-*N*-(4-iodophenyl)benzamide (see the Supporting Information (SI)).[21] The 3,4,5-tris(dodecyloxy)-N-(4-ethynylphenyl)benzamide group was chosen for its known ability to form robust supramolecular aggregates when grafted onto polyaromatic moieties in solution and in the solid state.[22] To accomplish enantioenriched (*P*) and (*M*) enantiomers of **1** and **2**, high-performance liquid chromatography (HPLC) enantiomeric resolution process was performed (see the Supporting Information for details). All the new compounds **1** and **2** were characterized by utilizing standard spectroscopic techniques (^{1}H NMR, ^{13}C NMR, and Fourier transform infrared (FTIR) spectroscopy and high-resolution mass spectrometry−electrospray ionization mass spectrometry (see the Supporting Information).

The self-assembling features of the reported [6]helicene **1** have been initially investigated by performing concentration dependent ^{1}H NMR experiments in $CDCl_3$ as solvent. The resonances of both the aromatic and aliphatic protons of the *M* enantiomer of the 2,15-disubstituted **1** remain unaltered upon increasing the concentration. On the contrary, the broad singlet corresponding to the amide protons deshields upon increasing the concentration (Figure 2a). These findings, coincident with that previously observed for both the racemic mixture or the enantioenriched sample of the 2,15-disubstituted helicene with four amide groups,[18] imply the non-covalent interaction of these units by the formation of a twofold array of H-bonding interactions between the amide functional groups. FTIR spectra in solution corroborate the formation of such arrays of H-bonding interactions. Indeed, the FTIR spectra of **1** in a good solvent like chloroform and at diluted experimental conditions (total concentration c_T = 1 mM), that favors the solvation of the monomeric species, displays the N-H and Amide I stretching bands at 3430 and 1676 cm^{-1}, respectively (Figure 2b). These wavenumbers, that are observed for both the racemic and the enantioenriched forms of compound **1**, are diagnostic to unbonded amide functional groups.[19,23] However, the N-H and Amide I stretching bands shift to lower wavenumbers (~3300 and 1647 cm^{-1}, respectively) by using methylcyclohexane (MCH) to register the corresponding FTIR spectra, a bad solvent that favors the self-assembly of nonpolar systems (Figure 2b). These wavenumbers observed in MCH are diagnostic of the operation of intermolecular H-bonding interactions between the amide functional groups.[19,23] A definitive clue on the self-assembling mode of the 2,15-disubstituted [6]helicene **1** has been unveiled by registering the ROESY spectrum in $CDCl_3$ at more concentrated experimental conditions (c_T = 20 mM). This ROESY spectrum shows clear intermolecular contacts between the peripheral aliphatic side chains and most of the aromatic protons that can be justified by considering a head-to-tail arrangement of the monomeric units reinforcing the intermolecular H-bonding interactions between the amide functional groups (Figure 1b and 2c). Atomic force microscopy (AFM) onto highly oriented pyrolyzed graphite (HOPG) has been utilized to visualize the morphology of the aggregated species formed by the self-assembly of the [6]helicene **1**. The AFM images of diluted solutions (c_T = 10 μM) of compound **1** in MCH shows the formation of a large number of nanoparticles with typical heights of 2.5 nm (Figure S5).

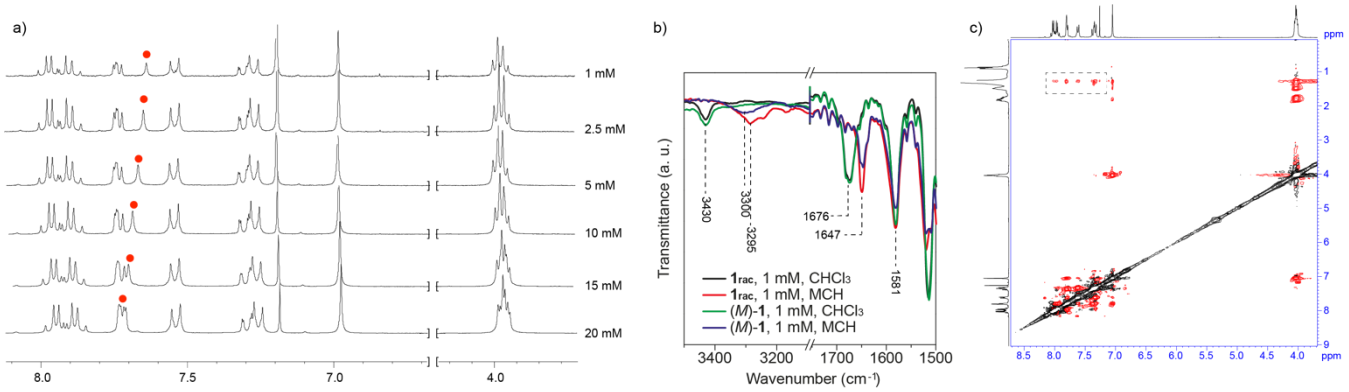

Figure 2. (a) Partial ^{1}H NMR spectra of (*M*)-**1** registered at different concentrations showing the aromatic and some of the aliphatic protons ($CDCl_3$, 300 MHz, 298 K). The red dot corresponds to the amide protons; b) Partial FTIR spectra of $\mathbf{1}_{rac}$ and (*M*)-**1** in $CHCl_3$ and MCH; c) ROESY NMR spectra ($CDCl_3$, 300 MHz, c_T = 20 mM; 293 K) of (*M*)-**1**. The dotted rectangle depicts the intermolecular through-space coupling signals between the aliphatic side chains and the aromatic resonances.

The self-assembling features of the 4,13-disubstituted [6]helicene **2** has been carried out by following a similar strategy to that performed by compound **1**. Thus, the concentration dependent ^{1}H NMR experiments carried out in $CDCl_3$ show the lack of any noticeable shift of the aromatic resonances but the slight shift of the broad singlet ascribable to the amide protons diagnostic of the negligible interaction of the π-surface of the [6]helicene and the operation of a twofold of H-bonding interactions between the amides (Figure S6). The intermolecular H-bonding interaction between the monomeric units is corroborated by registering the corresponding FTIR spectra in solution. Similarly to compound **1**, the NH and Amide I stretching bands of **2** in a diluted MCH solution (c_T = 1 mM) appear at 3275 and ~1645 cm^{-1}, respectively, clear signature of H-bonded amides.[19,23] However, the FTIR spectrum of **2** in $CHCl_3$ at c_T = 1 mM shows these stretching bands at ~3450 and ~1670 cm^{-1}, respectively, which imply that the amides are in a free state (Figure S7).[19,23] Interestingly, increasing the total concentration to 100 mM, the FTIR spectrum of **2** displays the presence of two NH stretching bands at ~3450 and 3330 cm^{-1} and two Amide I bands observed at ~1670 and ~1640 cm^{-1}, indicating that a part of the amide functions are engaged into H-bonded interactions (Figure S7). The presence of H-bonding interactions between the amide groups reveals a certain tendency of this helicene **2** to self-assemble at high concentrations. The ROESY spectrum of a concentrated solution (c_T = 20 mM) in $CDCl_3$ shows the lack of any short intermolecular contacts between the aromatic backbones and the aliphatic side chains (Figure S8). Therefore, and on the contrary to the head-to-tail arrangement of the monomeric unit to form the aggregated species of **1**, in the case of helicene **2** a head-to-head arrangement of the monomeric units in which the H-bonding interactions are slightly reinforced by the π-stacking of the helicene moieties, would result in organized, aggregated species (Figure 1c). These spectroscopic findings suggest that the 4,13-disubstituted helicene **2** self-assembles in a similar manner to its previously reported congener with four amides per monomeric unit.[18] However, the AFM images registered for compound **2** show the presence of nanoparticles with typical heights of less than 1 nm (Figure S9). This morphology observed for [6]helicene **2** contrasts with the fibrillar nature of the aggregated state of the previously reported congener of **2** endowed with four amide functional groups per monomeric units and reveals the strong impact of removing the flexible ethylene spacer between separating the [6]helicene core and the benzamide fragment.[18] Therefore, the presence of the 3,4,5-tris(dodecyloxy)-*N*-(4-ethynylphenyl)benzamide moieties, and more specifically, the steric effect exerted by the peripheral dodecyl side chains, prevents an efficient self-assembly of compound **2** that finally yields small aggregated species. This effect has been experimentally and theoretically demonstrated for some related π-conjugated systems endowed with these peripheral rigid segments for which self-assembly is an anticooperative supramolecular polymerization with a limited growth.[19,24]

Chiroptical and spin filtering properties. Since [6]helicenes are intrinsically chiral entities that exhibit remarkable chiroptical and emissive properties,[1,2,25] and the previously reported influence of self-assembly [6]helicenes on these properties,[18] we have performed a complete study of these features by performing electronic circular dichroism (ECD) and CPL measurements. Prior to investigate the chiroptical properties of these [6]helicenes, we have registered the UV-Vis spectra of both the racemic and enantioenriched forms of compound **1** in $CHCl_3$, a good solvent that favors the complete disassembly into monomeric species, and in MCH, a bad solvent that favors the aggregation of these monomeric units. In $CHCl_3$, both the racemic form and the enantioenriched sample show an identical absorption pattern with maxima at λ = 270 and 304 nm (Figure 3a). These findings are similar in MCH, in which both racemic and enantioenriched samples display identical UV-Vis spectra with maxima at λ = 270 and 299 nm (Figure 3a). The small hypsochromic effect observed in the UV-Vis spectra registered in MCH in comparison to those registered in $CHCl_3$ is indicative of a weak π-stacking of the non-planar [6]helicene moiety (Figure 3a). These subtle changes are also observed in the ECD spectra of the (*M*) and (*P*) enantiomers of [6]helicene **1** if $CHCl_3$ or MCH are utilized as solvents. Thus, these ECD spectra of both enantiomers are mirror image with maxima at 420, 375, 315, and 275 nm with zero crossing points at 340, 286, and 263 nm (Figure 3a). These subtle changes have been used to perform a solvent denaturation (SD) experiment to unravel the supramolecular polymerization mechanism. In these experiments, increasing amounts of the solution of an enantiomer in the good solvent are mixed with decreasing amounts of the same enantiomer in the bad solvent keeping the total concentration constant.[26] Unfortunately, the addition of tiny amounts of the $CHCl_3$ solution of (*M*)-**1** to the MCH solution to (*M*)-**1** at c_T = 10 μM results in a complete disassembly which

impedes the reliable derivation of the thermodynamic parameters associated to the supramolecular polymerization of these derivatives (Figure S10). These findings indicate the weak interaction between the monomeric units in the formation of the aggregates of [6]helicenes **1**.

The dichroic response of the *M* and *P* enantiomers of the 4,13-disubstituted helicene **2** in $CHCl_3$ shows mirror image ECD spectra with three Cotton effects at 368, 322, and 278 nm and zero crossing points at 349 and 295 nm (Figure 3c). These ECD spectra of the enantiomers of **2** are identical but slightly less intense in the bad solvent MCH, diagnostic of rather weak π-stacking of the contorted [6]helicene backbone (Figure 3c), behavior that strongly contrasts with that observed for the congener of **2** endowed with four amide functional groups per monomeric units. In these 4,13-disubstituted [6]helicenes, the efficient π-stacking of the aromatic moieties reinforced by the tetrafold array of amide H-bonds affords an efficient supramolecular polymerization in MCH that yields drastic changes in the corresponding ECD spectra with Cotton effects of opposite sign.[18] As stated before, the steric effect generated by the 3,4,5-tris(dodecyloxy)-*N*-(4-ethynylphenyl)benzamide moieties could be responsible for an anticooperative supramolecular polymerization mechanism attenuated by the growth that results in ECD spectra almost identical in both the good and bad solvents. [19,24]

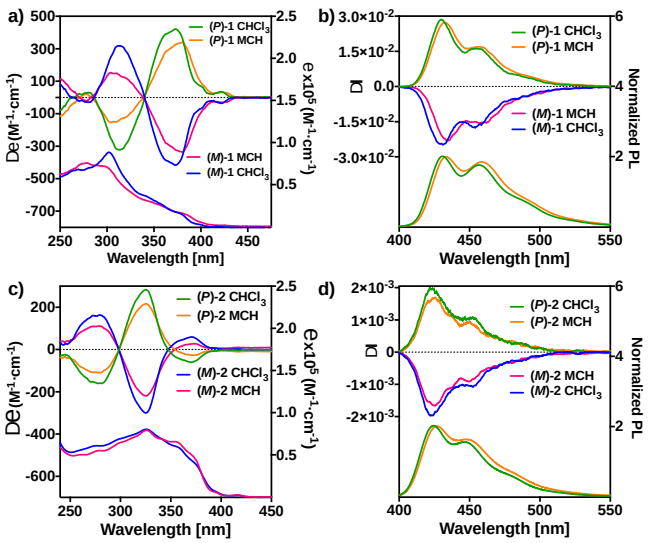

Figure 3. ECD (left axis) / UV−vis (right axis) (a) and CPL (left axis) / PL (right axis) (b) spectra of (*P*)-**1** and (*M*)-**1** in monomeric and aggregated states ($CHCl_3$ and MCH, respectively); ECD (left axis) / UV−vis (right axis) (c) and CPL (left axis) / PL (right axis) (d) spectra of (*P*)-**2** and (*M*)-**2** in monomeric and aggregated states ($CHCl_3$ and MCH, respectively). 'Normalized PL' stands for 'normalized photoluminescence'. Experimental conditions for UV−vis, ECD, CPL, and PL spectra: c_T = 10 μM and λ_{exc} = 365 nm.

To complement the investigation of the chiroptical properties of the enantiomers *M* and *P* of the reported [6]helicenes **1** and **2**, we have registered the CPL spectra of the enantiomers in the good solvent $CHCl_3$ and in the bad solvent MCH. The lack of an efficient π-stacking of the aromatic units in both **1** and **2** results in identical emission spectra for these two disubstituted [6]helicenes and for both solvents $CHCl_3$ and MCH with maxima at 430, 455, and 486 nm (λ_{exc} = 365 nm; Figure 3b and 3d). The corresponding CPL spectra are mirror image for the *M* and *P* enantiomers of **1** and **2**.

In addition, these CPL spectra are also identical in both the good and bad solvents thus conforming the weak supramolecular interaction between the monomeric units in the bad solvent (Figure 3b and 3d). The striking difference between the 2,15- and 4,13-disubstituted [6]helicenes **1** and **2** is the dissymmetry factor g_{lum}, defined as $g_{lum} = 2(I_L - I_R)/(I_L + I_R)$, I_L and I_R being the left- and right-handed luminescence emissions, respectively. In the case of the enantiomers of **1**, the g_{lum} values are $+2.8/-2.6 \times 10^{-2}$ (λ_{exc} = 365 nm) for (*P*)-**1** and (*M*)-**1**, respectively (Figure 3b). However, the g_{lum} values for [6]helicenes **2** are one order of magnitude lower ($+2.0/-2.0 \times 10^{-3}$; λ_{exc} = 365 nm in $CHCl_3$). These results are in line with previous investigations[18,20] on related compounds and confirm that the 2,15-substitution pattern is more favorable than the 4,13 one for aligning the electric and magnetic transition dipole moment and obtain strong CPL activity

Finally, we have also evaluated the spin polarization effect of the weakly self-assembled [6]helicenes **1** and **2.** This phenomenon is of crucial interest in the potential application of chiral systems in spintronics.[27] The spin selectivity of the electron transport through a chiral layer of the helicene-based polymer was carried out by magnetic conducting AFM (mc-AFM) measurements. For these investigations, the corresponding helicene was deposited on a gold-coated nickel substrate (Ni 100 nm and Au 8 nm), which can be magnetized with the north magnetic pole pointing toward the layer (up) or away from the layer (down) using an external magnetic field (Figure 4a). Furthermore, the nonmagnetic AFM tip was grounded, while the potential on the Au/Ni surface was varied. Despite dissimilar self-assembling features of the studied [6]helicenes similar spin polarization properties were observed for **1** and **2** aggregates, with the *M* and *P* enantiomers displaying a clear dependence of the current on the direction of the magnetization of the substrate. Thus, the spin selectivity of both enantiomers is controlled, in a reverse manner, by the applied magnetic field (see Figures 4a and 4b for **1** and Figures 4d and 4e for **2**). This spin selectivity corroborates the role of enantiopurity in spin-dependent transport properties as it has been demonstrated for the previously reported [6]helicenes[18] and some other chiral, self-assembled systems.[28] More details relevant to the room temperature mc-AFM experiments and averaging analysis is given in supporting information (see Figure-S12 and Figure-S13).

Finally, we have calculated the percentage of the spin polarization (SP%) by applying equation 1:

$$SP\% = (I_{up} - I_{down})/(I_{up} + I_{down}) \times 100 \qquad \text{Eq. 1}$$

In equation 1, I_{up} and I_{down} are the currents when the north pole of the magnetic field is directed upward or downward direction, respectively. The *SP%* calculated for the enantiomers of [6]helicenes **1** is 35% ± 8 (Figure 4c). These *SP%* values, even if lower than that registered for the [6]helicenes congeners previously reported,[18] are in the same range as that of some other self-assembled systems that present *SP%* values ranging from 6 to 40%[3] and are diagnostic of a higher polarizability of the supramolecular aggregated state.[29] These spin filtering properties imply that, upon applying the magnetic field in the up direction, *M* enantiomer selectively allows the electron spin to pass through the chiral layer, and vice versa, thus relating the absolute configuration of the helicene to the spin polarization and, therefore, the supramolecular non-covalent interaction of the monomeric species, together with the chemical structure of such

monomers, strongly affects the spin filtering effect. Similar behavior, with clear spin polarization within an average value of 40% ± 13 was observed in the case of (*P*) and (*M*)-**2** assemblies. Note that in these systems some variations were found in the I-V curves, especially in the case of the system **1** at around 2V, suggesting less stability of the assemblies and of the chiral layer at this voltage.

Interestingly, the two systems **1** and **2** display similar spin polarization values. It is worth to note that these SP values are averaged ones among 50 *I-V* curves. Furthermore, in past studies, we showed that the spin polarization is correlated with the disssymmetry factor of the molecules (see g_{abs} spectra on Figure S11). Hence it is possible that two molecules, despite having different structures, can show similar spin polarization.[30] However, all the parameters that control the final SP values are still not clearly understood.

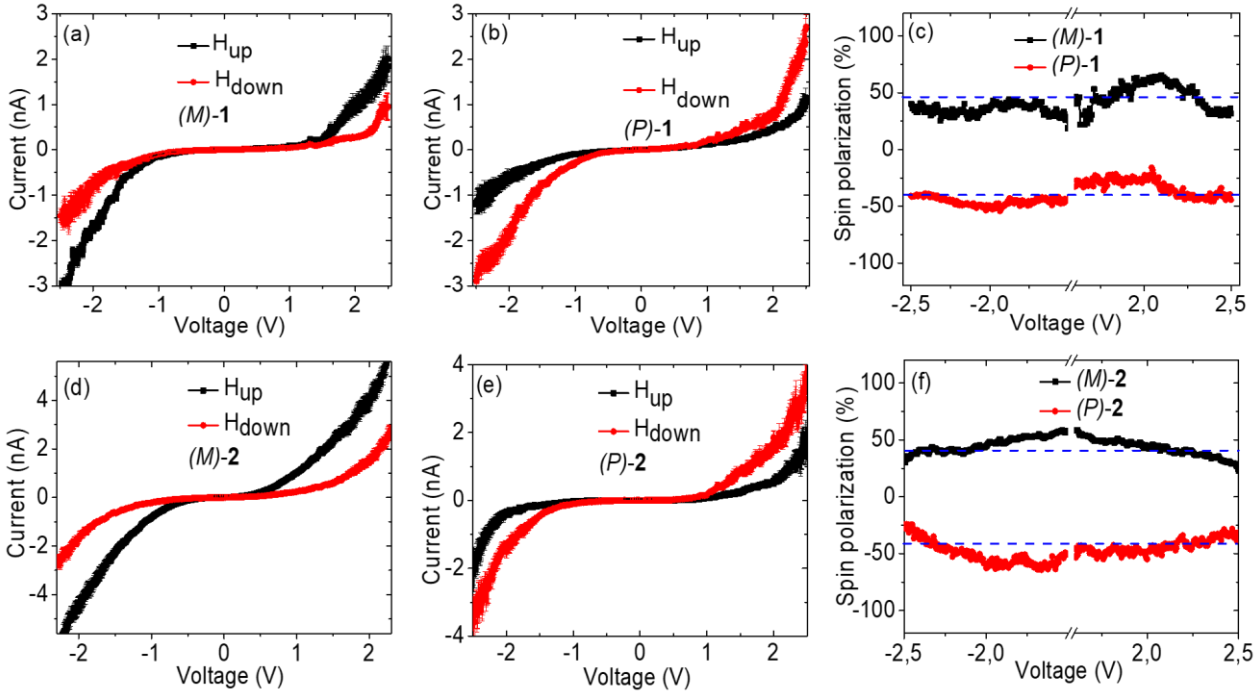

Figure 4. I-V curves recorded for (*M*)-**1** (a) and (*P*)-**1** (b) samples and for (*M*)-**2** (d) and (*P*)-**2** (e) samples with the magnet north pole pointing down (red) or up (black); spin polarization percentage (SP%) as a function of applied bias for (*M*)-**1** (black) and (*P*)-**1** (red) samples (c) and for (*M*)-**2** (black) and (*P*)-**1** (red) samples (f).

Conclusion

To conclude, we report herein on the self-assembling features and chiroptical activity and spin filtering properties of 2,15- and 4,13-disubstituted [6]helicenes decorated in their periphery with two 3,4,5-tris(dodecyloxy)-*N*-(4-ethynylphenyl)benzamide moieties (compounds **1** and **2**, respectively). These peripheral fragments provide with the ability of these contorted, chiral aromatic systems to generate aggregated species. The weak non-covalent interaction between these units conditions the corresponding CPL activity and spin polarization. The self-assembly is especially weak for 4,13-disubstituted [6]helicene **2** that, despite the formation of H-bonding interactions between the amide functional groups present in the peripheral moieties, present very similar chiroptical properties both in a good solvent ($CHCl_3$) or in a bad solvent (MCH) that favors the aggregation process. This effect could be accounted for by considering the steric effect that these groups could generate in the growing of the corresponding aggregate formed in a head-to-head fashion. Importantly, the self-assembling features of **1** and **2** also conditions the spin polarization properties with a clear spin filtering effect (with a spin polarization percentage of around 35-40%), for both systems. The results presented herein contribute to shed light on the structural elements participating in the achievement of functional, supramolecular polymers. Other aspects such as the influence of the optical purity (racemic vs. enantiopure) on the assembling properties of these systems is under current investigation.

Experimental Section

Synthesis of Compound 1

The corresponding bis-ethynyl-[6]helicene (*rac*-[6]helicene, 20 mg, 0.053 mmol, 1 eq.) and aryl iodide (3,4,5-tris(dodecyloxy)-*N*-(4-iodophenyl)benzamide (102 mg, 0.117 mmol, 2.2 eq.) were dissolved in 4 mL of a mixture of dry THF and Et_3N (1/1) and was degassed by 3 Vacuum/Ar cycles. CuI (1 mg, 0.0053 mmol, 0.1 eq.) and $Pd(PPh_3)_4$ (3.7 mg, 0.0053 mmol, 0.1 eq.) were added and the reaction mixture was stirred for 2 hours at 50ºC. The organic layer was evaporated under reduced pressure and the residue was purified by column chromatography (silica gel) using heptane/ethyl acetate (7/3). The fractions containing the product were evaporated under reduced pressure and the obtained compounds were purified by two recycling GPC cycles following the experimental conditions indicated in the general methods sections (see Supporting Information for details). **1** was obtained as a brown solid (65 mg, 87 %).

Synthesis of Compound 2

The corresponding bis-ethynyl-[6]helicene (*rac*-[6]helicene, 15 mg, 0.039 mmol, 1 eq.) and aryl iodide (3,4,5-tris(dodecyloxy)-*N*-(4-iodophenyl)benzamide (88 mg, 0.067 mmol, 2.5 eq.) were dissolved in 4 mL of a mixture of dry THF and Et_3N (1/1) and was degassed by 3 Vacuum/Ar cycles. CuI (0.7 mg, 0.0039 mmol, 0.1 eq.) and $Pd(PPh_3)_4$ (2.7 mg, 0.0039 mmol, 0.1 eq.) were added and the reaction mixture was stirred for 2 hours at 50ºC. The organic layer was evaporated under reduced pressure and the residue was purified by column chromatography (silica gel) using heptane/ethyl acetate (7/3). The fractions containing the product were evaporated under reduced pressure and the obtained compounds were purified by two recycling GPC cycles following the experimental conditions indicated in the general methods sections (see Supporting Information for details). **2** was obtained as a brown solid (65 mg, 63 %).

Additional experimental procedures and characterisation data are provided in Supporting Information.

The authors have cited additional references within the Supporting Information.[31,32]

Acknowledgements

Financial support by the MCIU of Spain (PID2020-113512GB-I00 and TED2021-130285B-I00) is acknowledged. R.R. thanks Xunta de Galicia for postdoctoral fellowship. R.N. acknowledges the partial support from the Israeli Ministry for Science and Technology. The European Commission Research Executive Agency (Grant Agreement number: 859752 − HEL4CHIROLED − H2020-MSCA-ITN-2019) is thanked for financial support. We acknowledge the Ministère de l'Education Nationale, de la Recherche et de la Technologie, the Centre National de la Recherche Scientifique (CNRS).

Keywords: helicenes • supramolecular assemblies • circularly polarized luminescence • chiral induced spin selectivity • spin polarization

[1] a) J. Crassous, I. G. Stará, I. Starý Helicenes - Synthesis, Properties and Applications, Wiley, **2022**; b) C.-F. Chen, Y. Shen, In Helicene Chemistry: From Synthesis to Applications; Springer: Berlin, Heidelberg, **2017**; c) M. Gingras, *Chem. Soc. Rev.* **2013**, *42*, 968−1006; d) M. Gingras, G. Felix, R. Peresutti, *Chem. Soc. Rev.* **2013**, *42*, 1007−1050; e) Y. Shen, C.-F. Chen, *Chem. Rev.* **2012**, *112*, 1463−1535; f) K. Dhbaibi, L. Favereau, J. Crassous, *Chem. Rev.* **2019**, *119*, 8846−8953.

[2] a) K. Dhbaibi, L. Abella, S. Meunier-Della-Gatta, T. Roisnel, N. Vanthuyne, B. Jamoussi, G. Pieters, B. Racine, E. Quesnel, J. Autschbach, J. Crassous, L. Favereau, *Chem. Sci.* **2021**, *12*, 5522−5533; b) M. J. Narcis, N. Takenaka, *Eur. J. Org. Chem.* **2014**, 21−34; c) D. Schweinfurth, M. Zalibera, M. Kathan, C. Shen, M. Mazzolini, N. Trapp, J. Crassous, G. Gescheidt, F. Diederich, *J. Am. Chem. Soc.* **2014**, *136*, 13045−13052; d) E. Anger, M. Srebro, N. Vanthuyne, L. Toupet, S. Rigaut, C. Roussel, J. Autschbach, J. Crassous, R. Réau, *J. Am. Chem. Soc.* **2012**, *134*, 15628−15631; e) T. Verbiest, S. V. Elshocht, M. Kauranen, L. Hellemans, J. Snauwaert, C. Nuckolls, T. J. Katz, A. Persoons, *Science* **1998**, *282*, 913−915.

[3] a) V. Kiran, S. P. Mathew, S. R. Cohen, I. Hernández Delgado, J. Lacour, R. Naaman, *Adv. Mater.* **2016**, *28*, 1957−1962; b) M. Kettner, V. Maslyuk, D. Ngrenberg, J. Seibel, R. Gutierrez, G. Cuniberti, K.-H. Ernst, H. Zacharias, *J. Phys. Chem. Lett.* **2018**, *9*, 2025−2030; c) T.-R. Pan, A.-M. Guo, Q.-F. Sun, *Phys. Rev. B: Condens. Matter Mater. Phys.* **2016**, *94*, No. 235448; d) A. M. García, C. Martínez, A. Ruiz-Carretero, *Front. Chem.* **2021**, *9*, 722727; e) Y. Liang, K. Banjac, K. Martin, N. Zigon, S. Lee, N. Vanthuyne, F. A. Garcés-Pineda, J. R. Galán-Mascarós, X. Hu, N. Avarvari, M. Lingenfelder, *Nature Comm.* **2022**, *13*, 3356.

[4] a) E. S. Gauthier, R. Rodríguez, J. Crassous, *Angew. Chem. Int. Ed*. **2020**, *59*, 22840-22856; b) B. Doisteau, J.-R. Jiménez, C. Piguet, *Front. Chem.* **2020**, *8*, 555; c) K. Staszak, K. Wieszczycka, V. Marturano, B. Tylkowski, *Coord. Chem. Rev.* **2019**, *397*, 76−90; d) R. Carr, N. H. Evans, D. Parker, *Chem. Soc. Rev.* **2012**, *41*, 7673−7686.

[5] a) S. Liu, F. Li, Y. X. Wang, X. J. Li, C. J.; Zhu, Y. X. Cheng, *J. Mater. Chem. C* **2017**, *5*, 6030−6036; b) E. M. Sánchez-Carnerero, F. Moreno, B. L. Maroto, A. R. Agarrabeitia, M. J. Ortiz, B. G. Vo, G. Muller, S. de la Moya, *J. Am. Chem. Soc.* **2014**, *136*, 3346−3349; c) Y. Haketa, Y. Bando, K. Takaishi, M. Uchiyama, A. Muranaka, M. Naito, H. Shibaguchi, T. Kawai, H. Maeda, *Angew. Chem., Int. Ed.* **2012**, *51*, 7967−7971; *Angew. Chem.* **2012**, *124*, 8091-8095.

[6] M. A. Medel, R. Tapia, V. Blanco, D. Miguel, S. P. Morcillo, A. G. Campaña, *Angew. Chem., Int. Ed.* **2021**, *60*, 6094−6100; *Angew. Chem.* **2021**, *133*, 6159-6165.

[7] J. Crassous, M. Fuchter, D. Freedman, N. Kotov, J. Moon, M. Beard, S. Feldmann *Nature Rev. Mater.* **2023**, *8*, 365–371.

[8] a) A. R. A. Palmans, E. W. Meijer, A. R. A. Palmans, E. W. Meijer, *Angew. Chem. Int. Ed.* **2007**, *46*, 8948–8968; *Angew. Chem.* **2007**, *119*, 9106–9126; b) Y. Dorca, E. E. Greciano, J. S. Valera, R. Gómez, L. Sánchez, *Chem. Eur. J.* **2019**, *25*, 5848–5864.

[9] C. Kulkarni, E. W. Meijer, A. R. A. Palmans, *Acc. Chem. Res.* **2017**, *50*, 1928−1936.

[10] a) S. Ghosh, X.-Q. Li, V. Stepanenko, F. Würthner, *Chem.−Eur. J.* **2008**, *14*, 11343−11357; b) M. A. Martínez, A. Doncel-Giménez, J. Cerdá, J. Calbo, R. Rodríguez, J. Aragó, J. Crassous, E. Ortí, L. Sánchez, *J. Am. Chem. Soc.* **2021**, *143*, 13281−13291; c) S. van Cleuvenbergen, P. Kedziora, J.-L. Fillaut, T. Verbiest, K. Clays, H. Akdas-Kilig, F. Camerel, *Angew. Chem. Int. Ed.* **2017**, *56*, 9546–9550; *Angew. Chem.* **2017**, *129*, 9674-9678.

[11] a) E. E. Greciano, J. Calbo, J. Buendía, J. Cerdá, J. Aragó, E. Ortí, L. Sánchez, *J. Am. Chem. Soc.* **2019**, *141*, 7463−7472; b) F. García, L. Sánchez, *J. Am. Chem. Soc.* **2012**, *134*, 734−742.

[12] a) N. Sasaki, M. F. J. Mabesoone, J. Kikkawa, T. Fukui, N. Shioya, T. Shimoaka, T. Hasegawa, H. Takagi, R. Haruki, N. Shimizu, S. Adachi, E. W. Meijer, M. Takeuchi, K. Sugiyasu, *Nat. Commun.* **2020**, *11*, 1−9; b) M. F. J. Mabesoone, A. J. Markvoort, M. Banno, T. Yamaguchi, F. Helmich, Y. Naito, E. Yashima, A. R. A. Palmans, E. W. Meijer, *J. Am. Chem. Soc.* **2018**, *140*, 7810−7819.

[13] M. M. J. Smulders, P. J. M. Stals, T. Mes, T. F. E. Paffen, A. P. H. J. Schenning, A. R. A. Palmans, E. W. Meijer, *J. Am. Chem. Soc.* **2010**, *132*, 620−626.

[14] M. L. Ślęczkowski, M. F. J. Mabesoone, P. Ślęczkowski, A. R. A. Palmans, E. W. Meijer, *Nat. Chem.* **2021**, *13*, 200−207.

[15] a) J. S. Kang, S. Kang, J. M. Suh, S. M. Park, D. K. Yoon, M. H. Lim, W. Y. Kim, M. Seo, *J. Am. Chem. Soc.* **2022**, *144*, 2657–2666; b) E. E. Greciano, R. Rodríguez, K. Maeda, L. Sánchez, *Chem. Commun.* **2020**, *56*, 2244−2247; c) J. Kim, J. Lee, W. Y. Kim, H. Kim, S. Lee, H. C. Lee, Y. S. Lee, M. Seo, S. Y. Kim, *Nat. Commun*. **2015**, *6*, 6959.

[16] a) Z. Xie, V. Stepanenko, K. Radacki, F. Würthner, *Chem. − Eur. J.* **2012**, *18*, 7060−7070; b) J. Buendía, E. E. Greciano, L. Sánchez, *J. Org. Chem.* **2015**, *80*, 12444−12452.

[17] a) K. E. S. Phillips, T. J. Katz, S. Jockusch, A. J. Lovinger, N. J. Turro, *J. Am. Chem. Soc.* **2001**, *123*, 11899−11907; b) T. Kaseyama, S. Furumi, X. Zhang, K. Tanaka, M. Takeuchi, *Angew. Chem., Int. Ed.* **2011**, *50*, 3684−3687; *Angew. Chem.* **2011**, *123*, 3768–3771; c) J. S. Valera, R. Gómez, L. Sánchez, *Org. Lett.* **2018**, *20*, 2020−2023; for a review on supramolecular assemblies of chiral molecules devoid of chiral centers see: d) W. R. Henderson, R. K. Castellano, *Polym. Int.* **2021**, *70*, 897–910.

[18] R. Rodríguez, C. Naranjo, A. Kumar, P. Matozzo, T. Kumar Das, Q. Zhu, N. Vanthuyne, R. Gómez, R. Naaman, L. Sánchez, J. Crassous, *J. Am. Chem. Soc.* **2022**, *144*, 7709−7719.

[19] Y. Dorca, C. Naranjo, G. Ghosh, B. Soberats, J. Calbo, E. Ortí, G. Fernández, L. Sánchez, *Chem. Sci.*, **2022**, *13*, 81–89.

[20] a) E. Anger, M. Srebro, N. Vanthuyne, L. Toupet, S. Rigaut, C. Roussel, J. Autschbach, J. Crassous, R. Réau, *J. Am. Chem. Soc.* **2012**, *134*,

15628–15631; b) C. Shen, F. Gan, G. Zhang, Y. Ding, J. Wang, R. Wang, J. Crassous, H. Qiu, *Mater. Chem. Front.* **2020**, *4*, 837−844.

[21] F. Wang, M. A. J. Gillissen, P. J. M. Stals, A. R. A. Palmans, E. W. Meijer, *Chem. Eur. J.* **2012**, *18*, 11761–11770.

[22] S. Diring, F. Camerel, B. Donnio, T. Dintzer, S. Toffanin, R. Capelli, M. Muccini, R. Ziessel, *J. Am. Chem. Soc.* **2009**, *131*, 18177-18185.

[23] a) M. Wehner, M. I. S. Röhr, M. Bühler, V. Stepanenko, W. Wagner, F. Würthner, *J. Am. Chem. Soc*. **2019**, *141*, 6092-6107; b) D. S. Philips, K. K. Kartha, A. T. Politi, T. Krüger, R. Q. Albuquerque, G. Fernández, *Angew. Chem. Int. Ed*. **2019**, *58*, 4732-4736; *Angew. Chem.* **2019,** *131*, 4782-4787; c) E. E. Greciano, S. Alsina, G. Ghosh, G. Fernández, L. Sánchez, *Small Methods* **2020**, *4*, 1900715.

[24] R. van der Weegen, P. A. Korevaar, P. Voudouris, I. K. Voets, T. F. A. de Greef, J. A. J. M. Vekemans, E. W. Meijer, *Chem. Commun*. **2013**, *49*, 5532-5534.

[25] K. Dhbaibi, M. Grasser, H. Douib, V. Dorcet, O. Cador, N. Vanthuyne, F. Riobé, O. Maury, S. Guy, A. Bensalah-Ledoux, B. Baguenard, G. L J A Rikken, C. Train, B. Le Guennic, F. Pointillart, M. Atzori, J. Crassous *Angew. Chem. Int. Ed*. **2023**, e202215558; *Angew. Chem.* **2023***,* e202215558.

[26] P. A. Korevaar, C. Schaefer, T. F. A. de Greef, E. W. Meijer, *J. Am. Chem. Soc.* **2012**, *134*, 13482−13491.

[27] a) K. Banerjee-Ghosh, O. Ben Dor, F. Tassinari, E. Capua, S. Yochelis, A. Capua, S.-H. Yang, S. S. P. Parkin, S. Sarkar, L. Kronik, L. T. Baczewski, R. Naaman, Y. Paltiel, *Science* **2018**, *360*, 1331−1334; b) R. Naaman, Y. Paltiel, D. H. Waldeck, *Nat. Rev. Chem.* **2019**, *3*, 250−260; c) Y.-H. Kim, Y. Zhai, H. Lu, X. Pan, C. Xiao, E. A. Gaulding, S. P. Harvey, J. J. Berry, Z. V. Vardeny, J. M. Luther, C. M. Beard, *Science* **2021**, *371*, 1129−1133; d) H. Lu, J. Wang, C. Xiao, X. Pan, X. Chen, R. Brunecky, J. J. Berry, K. Zhu, M. C. Beard, Z. V. Vardeny, *Sci. Adv.* **2019**, *5*, No. eaay0571.

[28] a) Y. Sang, Q. Zhu, X. Zhou, Y. Jiang, M. Liu, *Angew. Chem. Int. Ed*. **2023**, DOI:10.1002/anie.202215867; b) A. K. Mondal, N. Brown, S. Mishra, P. Makam, D. Wing, S. Gilead, Y. Wiesenfeld, G. Leitus, L. J. W. Shimon, R. Carmieli, D. Ehre, G. Kamieniarz, J. Fransson, O. Hod, L. Kronik, E. Gazit, R. Naaman, *ACS Nano* **2020**, *14*, 16624; c) S. Mishra, A. K. Mondal, S. Pal, T. K. Das, E. Z. B. Smolinsky, G. Siligardi, R. Naaman, *J. Phys. Chem. C* **2020**, *124*, 10776; d) A. Kumar Mondal, M. D. Preuss, M. L. Ślęczkowski, T. Kumar Das, G. Vantomme, E. W. Meijer, R. Naaman, *J. Am. Chem. Soc.* **2021**, *143*, 7189−7195.

[29] a) J. Fransson, *Phys. Rev. B* **2020**, *102*, No. 235416; b) T. K. Das, F. Tassinari, R. Naaman, J. Fransson, *J. Phys. Chem. C* **2022**, *126*, 3257−3264.

[30] D. Amsallem, A. Kumar, R. Naaman, O. Gidron, *Chirality* **2023**, *35*, 562−568.

[31] A. U. Malik, F. Gan, C. Shen, N. Yu, R. Wang, J. Crassous, M. Shu, H. Qiu, *J. Am. Chem. Soc.,* **2018**, *140*, 2769-2772.

[32] K. Dhbaibi, L. Favereau, M. Srebro-Hooper, C. Quinton, N. Vanthuyne, L. Arrico, T. Roisnel, B. Jamoussi, C. Poriel, C. Cabanetos, J. Autschbach, J. Crassous, *Chem. Sci.,* **2020**, *22*, 567-576.

Entry for the Table of Contents

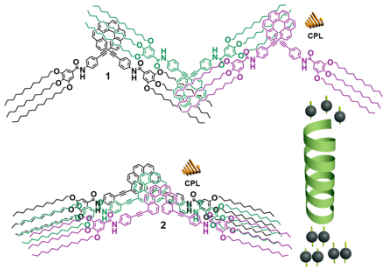

Carbo[6]helicenes decorated with 3,4,5-tris(dodecyloxy)-*N*-(4-ethynylphenyl)benzamide moieties at their periphery give access to self-assemblies with circularly polarized luminescence and spin selectivity.

Institute and/or researcher Twitter usernames: @LSM_LAB, @JeanneCrassous